An accurate colon residue detection algorithm with partial volume segmentation

Xiang li[1], Zhengrong Liang[2], Pengpeng Zhang[1] and Gerald J. Kutcher[1]
Department of Radiation Oncology, Columbia University[1]
Department of Radiology, State University of New York at Stony Brook[2]

Abstract: Colon cancer is the second leading cause of cancer-related death in the United States. Earlier detection and removal of polyps can dramatically reduce the chance of developing malignant tumor. Due to some limitations of optical colonoscopy used in clinic, many researchers have developed virtual colonoscopy as an alternative technique, in which accurate colon segmentation is crucial. However, partial volume effect and existence of residue make it very challenging. The electronic colon cleaning technique proposed by Chen *et al* is a very attractive method, which is also kind of hard segmentation method. As mentioned in their paper, some artifacts were produced, which might affect the accurate colon reconstruction. In our paper, instead of labeling each voxel with a unique label or tissue type, the percentage of different tissues within each voxel, which we call a mixture, was considered in establishing a maximum *a posterior* probability (MAP) image-segmentation framework. A Markov random field (MRF) model was developed to reflect the prior probability for the tissue mixtures. The spatial information based on hard segmentation was used to determine which tissue types are in the specific voxel. Parameters of each tissue class were estimated by the expectation-maximization (EM) algorithm during the MAP tissue-mixture segmentation. Real CT experimental results demonstrated that the partial volume effects between four tissue types have been precisely detected. Meanwhile, the residue has been electronically removed and very smooth and clean interface along the colon wall has been obtained.

Keywords: Virtual Colonoscopy, Partial Volume Segmentation, Markov Random Field

I. Introduction

Colon cancer is the second leading cause of cancer-related death in the United States [1]. Earlier detection and removal of polyps can dramatically reduce the chance of developing malignant tumor. Currently, the optical colonoscopy is widely used in clinical practice. However, this technique is an invasive method that requires the intravenous sedation, approximately one-hour operation and costs a lot. Many researchers have developed virtual colonoscopy as an alternative technique [2]-[6]. A computer system is used to navigate the entire colon structure reconstructed from a patient's abdominal CT images. This method requires a very clean colon lumen. The electronic colon cleaning technique [8] proposed by Chen *et al* is a very attractive method. However, their method (adaptive Vector Quantirization algorithm [7]) is a kind of hard segmentation. The partial volume (PV) effects are not fully taken into account in their method. In the real colon CT image, there are many types of partial volume effect. In Chen's method two partial volume effects: air and soft tissue, soft tissue and residue, have been considered. Therefore, the soft tissue layer between air and residue, which should be not existent, has been incorrectly segmented. After segmentation, distance criterion between colon and residue was used to eliminate this layer. As mentioned in their paper, some artifacts were produced, which might affect the accurate colon reconstruction. The objective of our paper is to propose a more accurate partial volume segmentation method to remove the residue and reduce the artifacts in order to obtain a more accurate colon lumen.

In our previous work the fully partial volume segmentation algorithm has been proposed to segment the multi-spectrum magnetic resonance images [17]. But it might not suitable for the colon CT images. In this paper, a more strict prior model is presented to determine the type of the partial volume effect. The organization of this paper is as follows. Section II presented a framework for the automated partial volume segmentation algorithm. The section III showed the volunteer's results, and section IV described the conclusion and further works.

For correspondence: xl2112@Columbia.edu, Tel. (212)-3059490

Medical Imaging 2004: Image Processing, edited by J. Michael Fitzpatrick, Milan Sonka, Proceedings of SPIE Vol. 5370 (SPIE, Bellingham, WA, 2004)
1605-7422/04/$15 doi: 10.1117/12.535230

II. Theory

In this section, first we are briefly reviewing our old fully partial volume segmentation algorithm, which is the theoretical basis of the whole work. Then, we will describe how the spatial information is used to improve the prior model in previous work. Finally, the flow chart will be presented.

A. PV Image Model

Let Γ and S be two sets: $\Gamma = \{1,2,\cdots,K\}$, and $S = \{1,2,\cdots,N\}$, where K is the total number of tissue classes and N is the total number of voxels in the acquired image. Let $\boldsymbol{Y}$ be a set of random variables, which represent the observed image intensities $Y = \{y_1,\cdots,y_i,\cdots y_N \,|\, i \in S\}$, and M be a set of vectors $M = \{m_1,\cdots,m_i,\cdots,m_N \,|\, i \in S\}$ with the following properties of (a) $m_i = (m_{i1},\ldots,m_{ik})$, $k \in \Gamma$, and (b) $\sum_{k=1}^{K} m_{ik} = 1$, $0 \le m_{ik} \le 1$, where m_{ik} reflects the fraction of tissue type k inside voxel i. Each voxel value y_i in the observed image is considered as the following random process:

$$y_i = \sum_{k=1}^{K} m_{ik}\mu_k + \varepsilon_i \qquad (1)$$

where μ_k is the observed mean value of tissue type or class k when it fully fills in a voxel; m_{ik} can be defined as the probability of voxel i belonging to class k [15]; and ε_i is assumed as Gaussian noise associated with the observation y_i at voxel i with its mean being zero and variance of ν_i.

B. PV Image Segmentation

In order to estimate the mixture vectors M, given the observed image $\boldsymbol{Y}$, the statistically optimal MAP principle is used. We assume that the observation at each voxel is independent from the observations of other voxels, while the underline tissue distribution follows a MRF process, so that the conditional probability of the observed image $\boldsymbol{Y}$, given mixture M, can be simply expressed as

$$P(Y|M,\Phi) = \prod_{i=1}^{N} p(y_i|m_i,\Phi) = \prod_{i=1}^{N} \left(\frac{1}{2\pi\nu_i}\right)^{\frac{1}{2}} \exp\left[-\frac{(y_i - \mu^T m_i)^2}{2\nu_i}\right] \qquad (2)$$

where Φ is the parameter set $\{\mu_k, \nu_i, k \in \Gamma, i \in S\}$.

According to the MAP principle, the PV segmentation can be achieved by maximizing the posterior distribution, which is proportional to the joint distribution

$$P(M|Y,\Phi) = \frac{P(Y|M,\Phi)P(M|\Phi)}{P(Y|\Phi)} \propto P(Y|M,\Phi)P(M|\Phi) \qquad (3)$$

Markov Random Field (MRF) theory has been widely used in hard segmentation [9]-[13]. In this paper a MRF model has been used to define the prior distribution of mixture M, which is also adopted by Choi *et al* [14].

$$p(m_i|N_i) = \frac{1}{Z}\exp\left(-\alpha \sum_{j \in N_i} \kappa_j \left\| m_i - m_j \right\|^2\right) \qquad (4)$$

where N_i denotes the neighborhood of voxel i, α is a parameter controlling the degree of the smooth penalty on the mixture M, κ_j is a scale factor reflecting the difference among different orders of the neighbors, and Z is the normalization factor for the MRF model. In this paper, only the first-order neighborhood system is used.

In searching for the solution for maximizing the posterior probability of equation (3), the well-established iterated conditional modes (ICM) algorithm was utilized in this paper. Equivalently, the solution is determined by minimizing the posterior energy function of

$$U=\frac{1}{2\nu_i}(y_i-\mu^T m_i)^2+\alpha\sum_{j\in N_i}\kappa_j\left\|m_i-m_j\right\|^2 \tag{5}$$

Equation (5) has a quadratic property. So we can rewrite it as follows

$$U=\frac{1}{2}m_i^T A m_i+b^T m_i+C \tag{6}$$

$$A=[\frac{\mu\mu^T}{\nu_i}+2\alpha\sum_{j\in N_i}\kappa_j I] \tag{7}$$

$$b^T=-\frac{y_i}{\nu_i}\mu^T-2\alpha\sum_{j\in N_i}\kappa_j m_j^T \tag{8}$$

where *C* is a constant and *I* is an identity matrix. Given the smoothing properties of mixture m_i, the solution of minimizing function (5) is unique.

Performance of the PV segmentation on minimizing equation (5) strongly depends on an accurate estimation of the model parameter set Φ or (μ_k, ν_i). In the next section, we employ the EM algorithm [16] to estimate the model parameters Φ.

C. Parameter Estimation

Within each voxel volume, there are possibly *K* tissue types, where each tissue type has a contribution to that observed voxel value y_i. Let x_{ik} be the contribution of tissue type *k* to the observation y_i. Assuming that x_{ik} follows a Gaussian distribution and all tissue types are not correlated each other, we have the following equation of

$$y_i=\sum_{k=1}^{K}x_{ik}\ . \tag{9}$$

The conditional probability of x_{ik} given the parameter set Φ is distributed following a normal functional $N(m_{ik}\mu_k, m_{ik}\sigma_k)$, where σ_k is the variance of observing tissue type *k* when it fully fills a voxel. This σ_k definition implies that the variance ν_i of observing the mixture voxels is smooth over the whole image volume and has the following property of $\nu_i=\sum_{k=1}^{K}m_{ik}\sigma_k$ for each voxel *i*. When voxel *i* is fully filled by a same tissue type *k*, then $\nu_i=\sigma_k$. A similar definition for the relation of ν_i and σ_k, as well as the probability function for x_{ik}, were reported in Leemput's work in terms of down sampling [14].

By the EM terminology, an observation y_i is a random variable, which is incomplete in reflecting the underline true information, while x_{ik} is an unobservable random variable and reflects the complete information for each underline tissue process. The EM algorithm seeks a solution for the model parameters Φ, now they include both μ_k and σ_k, via the complete sampling density by interleaved Expectation and Maximization steps in an iterative manner.

The E-step computes the conditional complete-sampling density, given the observed data ***Y*** and the *n*-th iterated estimate of the model parameter $\Phi^{(n)}$

$$Q(\Phi|\Phi^{(n)})=\mathrm{E}[\ln P(\mathbf{X}|\Phi)|\mathbf{Y},\Phi^{(n)}]=-\tfrac{1}{2}\sum_{i,k}[\ln(2\pi)+\ln(m_{ik}\sigma_k)+\frac{1}{m_{ik}\sigma_k}(x_{ik}^{2(n)}-2m_{ik}\mu_k x_{ik}^{(n)}+m_{ik}^2\mu_k^2)] \tag{10}$$

where the conditional means for x_{ik} and x_{ik}^2 are given below

$$x_{ik}^{(n)} = \mathrm{E}[x_{ik} \mid y_i, \Phi^{(n)}] = m_{ik}\mu_k^{(n)} + \frac{m_{ik}\sigma_k^{(n)}}{\sum_{j=1}^{K} m_{ij}\sigma_j^{(n)}} \cdot (y_i - \sum_{j=1}^{K} m_{ij}\mu_j^{(n)}) \tag{11}$$

$$x_{ik}^{2(n)} = \mathrm{E}[x_{ik}^2 \mid y_i, \Phi^{(n)}] = x_{ik}^{(n)2} + m_{ik}\sigma_k^{(n)} \frac{\sum_{j\neq k}^{K} m_{ij}\sigma_j^{(n)}}{\sum_{j=1}^{K} m_{ij}\sigma_j^{(n)}} \tag{12}$$

The M-step determines the (n+1)-th iterated estimate, which maximizes the conditional complete-sampling density of equation (10).

For parameter μ_k we have:

$$\mu_k^{(n+1)} = \frac{\sum_i x_{ik}^{(n)}}{\sum_i m_{ik}} \cdot \tag{13}$$

For parameter σ_k, we have:

$$\sigma_k^{(n+1)} = \frac{1}{N}\sum_i \frac{(x_{ik}^{2(n)} - 2m_{ik}\mu_k^{(n+1)}x_{ik}^{(n)} + m_{ik}^2\mu_k^{(n+1)2})}{m_{ik}} = \frac{1}{N}\sum_i \{m_{ik}[\mu_k^{(n)} - \mu_k^{(n+1)} + \frac{\sigma_k^{(n)}(y_i - \sum_{j=1}^{K} m_{ij}\mu_j^{(n)})}{\sum_{j=1}^{K} m_{ij}\sigma_j^{(n)}}]^2 + \frac{\sigma_k^{(n)}\sum_{j\neq k}^{K} m_{ij}\sigma_j^{(n)}}{\sum_{j=1}^{K} m_{ij}\sigma_j^{(n)}}\} \tag{14}$$

D. Determination of Partial Volume effect

The prior model described in equation (4) is generally applicable to the situation, in which there can be any number of tissue types in each voxel. For the colon CT image, there are four tissue types: air, soft tissue, muscle and bone (or enhanced residue). As a matter of fact, it is impossible that every voxel contain four tissue types. All the possible partial volume effects have been shown in table 1. The performance of partial volume segmentation depends on the accuracy of the prior model. In this paper, the spatial information is used to determine which tissue types in each voxel. In figure1, the black spot represents the current voxel. Our partial volume segmentation algorithm is an iterative method. After each iteration, the partial volume segmentation results can be easily transferred into hard segmentation by labeling the voxel with the tissue type, which has the largest mixture value in this voxel. By using hard segmentation results, the tissue types of the neighborhood voxels of the current voxel (as seen in figure1, totally 32 voxels) determine which tissue types in this voxel. For example, if the current voxel is surrounded by bone, fat and air, we assume that this voxel is filled with those three tissue types. In this paper, we follow the exact rules as table 1 except index 1and 4. If the current voxel is surrounded only by air or bone, we assign this voxel with partial volume effect index 5 or 9.

Table 1. Partial volume effect classes index

Index	Tissue types	Index	Tissue types
1	Air only	9	Tissue and bone
2	Tissue only	10	Muscle and bone
3	Muscle only	11	Air, tissue and muscle
4	Bone only	12	Air, tissue and bone
5	Air and tissue	13	Air, muscle and bone
6	Air and muscle	14	Tissue and muscle and bone
7	Air and bone	15	Air, tissue, muscle and bone
8	Tissue and muscle		

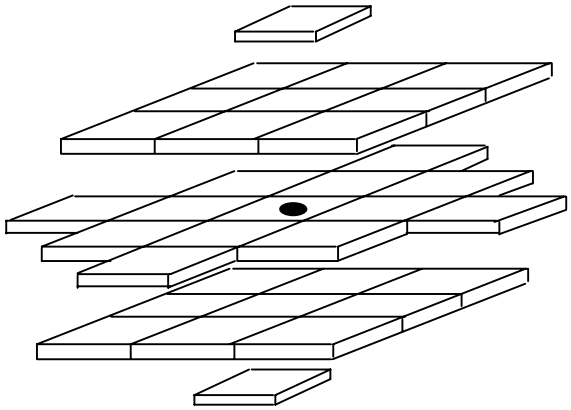

Figure1. Neighborhood system diagram.

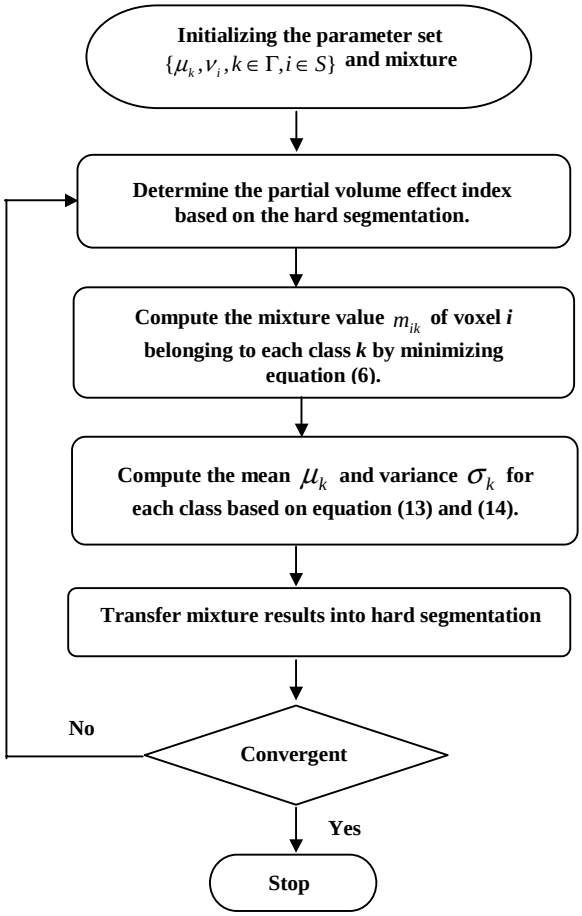

Figure2. The flow chart of the whole algorithm

In summary, our PV segmentation algorithm can be implemented by the flow chart shown in figure2. For the initialization, we just adopt the simple threshold algorithm to perform the hard segmentation and parameter estimation, then transfer hard segmentation result into mixture *M* by initializing each voxel 100% belonging to a specific tissue type. In addition, the termination criterion was defined as:

$$Max\left(\left|1-\frac{\mu_k^{(n+1)}}{\mu_k^{(n)}}\right|, k \in \Gamma\right) \le \varepsilon \qquad (15)$$

Where when the maximum difference between the means of each class at the (n)-th and (n+1)-th iterations is less than the specified threshold ε, the iteration process will be terminated. In this paper, ε was set to be 0.05. Our experimental results shows four iteration usually is good enough.

III. Results

In this study, seven volunteers have been tested to evaluate our new algorithm. Before obtaining CT images, the volunteer was asked to take at least one-day soft-food diet (yogurt, cereal, mashed potatoes, etc). In order to enhance the residual materials, the patient also ingests four 250cc doses of 2.1% w/v barium sulfate suspension with meals, as well as two doses of 60cc of gastroview (diatrizoate meglumine and diatrizoate sodium solution) during the night before and the morning of the procedure. After the patient's colon is inflated with CO2 through a small bore rectal tube, CT images are obtained by using standard virtual colonoscopy parameters.

A high speed helical CT scanner (HiSpeed CT/I, GE Medical Systems, Milwaukee, WI) was used to acquire the abdominal images. The image protocol parameters are: 120kVp, 60-120 mA (reduced dose to volunteer), 512x512 array field of view, 1.5-2.0:1 pitch and 3-5 mm collimation. The scanning time ranges from 30 to 40 seconds. Raw data were reconstructed at 1mm intervals. Depending on the height of each volunteer, 300-450 slice images were acquired.

Figure3a showed the volunteer's colon CT image. It is clearly seen that there are a lot of residue inside the colon. The existence of residue hinders the interpretation of the whole colon structure. By using our new partial volume segmentation algorithm, the residue can be accurately detected and electronically removed. Meanwhile, the partial volume effect between air and soft tissue (after the removal of residue) has been maintained. Figure3.b showed the colon CT image after processing.

Figure4a was the hard segmentation results transferred from mixture segmentation. It is very clearly seen that the great details of the colon wall have been missed due to the partial volume effect. Figure 4b showed mixture of the colon lumen, which includes the more information than the hard segmentation.

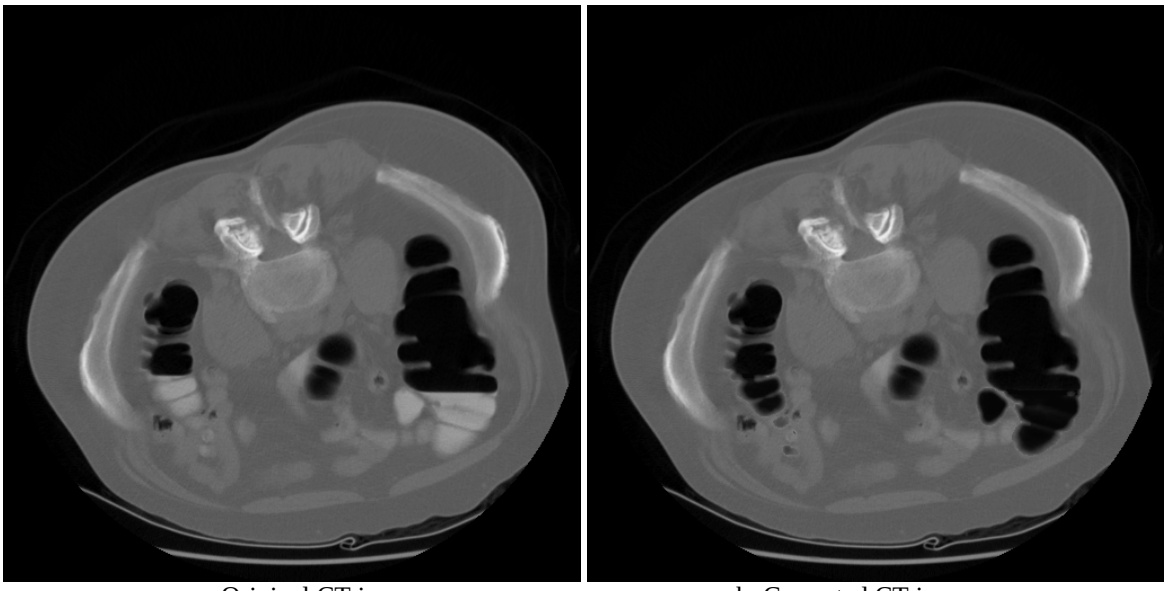

a. Original CT image b. Corrected CT image

Figure3. Electronic removal of residue.

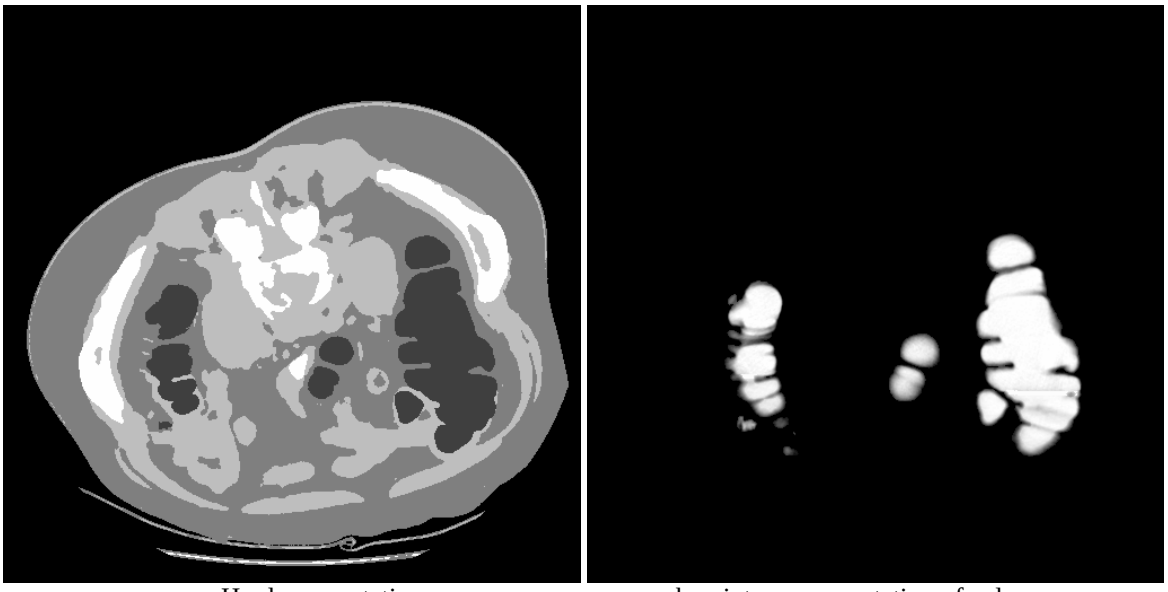

a. Hard segmentation b. mixture segmentation of colon

Figure4. Segmentation

IV. Conclusion

In this paper we proposed a new fully partial volume segmentation algorithm. The hard segmentation results were used to determine the type of the partial volume effect. Real CT experimental results demonstrated that the partial volume effects have been precisely detected. Meanwhile, the residue has been electronically removed and very smooth and clean interface along the colon wall has been obtained. The mixture segmentation provided the more information about the colon lumen than the hard segmentation. How to use those information to do the automatic polyps detection is in progress.

V. Reference

[1] "Cancer facts and figures", *Amer. Cancer Soc.*, Atlanta, GA, 2003.

[2] R. M. Summers, C. F. Beaulieu, L. M. Pusanik, J. D. Malley, *et al.*, " Automated Polyp Detection at CT colonoscopy: Feasibility Study", Radiology, 216(1), pp.284-290, July, 2000.

[3] R. M. Summers, C. D. Johnson, L. M. Pusanik, J.D. Malley, *et al.*, "Automated Polyp Detection at CT colonoscopy: Feasibility Assessment in a Human Population", Radiology, 219(1), pp.51-59, April, 2001.

[4] Hiroyuki Yoshida and Janne nappi, "Three-Dimensional Computer-Aided Diagnosis Scheme for Detection of Colonic Polyps", *IEEE Trans. Med. Imag*., vol. 20, pp. 1261-1274, Dec, 2001.

[5] Hiroyuki Yoshida, Yoshitaka Masutani, Peter Maceneaney, David T. Rubin, Abraham H. Dachman, " Computerized Detection of Colonic Polyps at CT colonoscopy on the Basis of Volumetric Features: Pilot Study", Radiology, 222(2), pp.327-336, Feb, 2002.

[6] Zhengrong Liang, "Virtual Colonoscopy: An Alternative Approach to Examination of the Entire Colon", INNERVISION, 16, pp.40-44, 2001.

[7] D. Chen, L. Li and Z. Liang, "A self-adaptive vector quantization algorithm for MR image segmentation", *Proc. Intl Society Magnetic Resonance Medicine*, 1999.

[8] D. Chen, Z. Liang, M. R. Wax, L. Li, B. Li and A. E. Kaufman, "A novel approach to extract colon lumen from CT image for virtual colonoscopy", *IEEE Trans. Med. Imag.*, vol. 19 (12), pp. 1220-1226, 2000.

[9] Z. Liang, J. R. Macfall, and D. P. Harrington, "Parameter estimation and tissue segmentation from multispectral MR images," *IEEE Trans. Med. Imag*., vol. 13, pp. 441-449, Sept, 1994.

[10] Z. Liang, R. J. Jaszczak, and R. E. Coleman, "Parameter estimation of finite mixtures using the EM algorithm and information criteria with application to medical image processing," *IEEE Trans. Nucl. Sci.*, vol. 39, pp. 1126-1133, 1992.

[11] Y. Zhang, M. Brady, and S. Smith, “Segmentation of brain MR images through a hidden markov random field model and expectation-maximization algorithm”, *IEEE Trans. Med. Imag.*, vol. 20, pp. 45-57, 2001.
[12] W. M. Wells III, W. E. L. Grimson, R. Kikinis, and F. A. Jolesz, “Adaptive segmentation of MRI data”, *IEEE Trans. Med. Imag.*, vol. 15, pp. 429-442, 1996.
[13] K. V. Leemput, F. Maes, D. Vandermeulen, and P. Suetens, “Automated model-based tissue classification of MR images of the brain,” *IEEE Trans. Med. Imag.*, vol. 18, pp. 897-908, 1999.
[14] H. S. Choi, D. R. Haynor, and Y. Kim, “Partial volume tissue classification of multichannel magnetic resonance images- A mixel model,” *IEEE Trans. Med. Imag.*, vol. 10, pp. 395-407, Sept, 1991.
[15]. K. V. Leemput, F. Maes, D. Vandermeulen, and P. Suetens, “A unifying framework for partial volume segmentation of brain MR images,” *IEEE Trans. Med. Imag*., vol. 22, pp. 105-119, Jan, 2003.
[16] A. Dempster, N. Laird, and D. Rubin, “Maximum likelihood from incomplete data via the EM algorithm”, *J R Stat. Soc*., vol. 39B, pp. 1-38, 1977.
[17] X. Li, L. Li, D. Eremina and Z. Liang, “Partial volume segmentation of medical images”,